JOURNAL OF PROPULSION AND POWER
Vol. 21, No. 4, July–August 2005

Oxidizer and Pressure Effects on the Combustion of 10-μm Aluminum Particles

Tim Bazyn,* Herman Krier,† and Nick Glumac‡
University of Illinois at Urbana–Champaign, Urbana, Illinois 61801

An experimental investigation of the combustion times of nominally 10-μm spherical aluminum particles burning in a shock tube is presented. Burn times were measured by observing the light emission from AlO, a combustion intermediate, at elevated ambient temperatures (~2650 K) while independently varying both oxidizer composition (O_2, CO_2, and H_2O in Ar) and pressure (3–30 atm). Burn times decreased with increasing oxidizer mole fraction for all oxidizers. The oxidizer species had a strong effect on the burn time, with oxygen giving the shortest burn times, followed by carbon dioxide and then water vapor. Burn times in CO_2 and H_2O were found to increase weakly with increasing pressure, while burn times in oxygen decreased as pressure increased. At the small particle sizes investigated here, there is some evidence that surface processes could be playing an important role in the overall rate of aluminum combustion.

Introduction

ALUMINUM is often added to solid-rocket-motor (SRM) propellants to increase chamber temperatures and mitigate combustion instabilities. When operating in SRMs, the aluminum passes through the primary flame zone of the propellant and reacts with the postflame gases, which consist primarily of H_2O, CO_2, and HCl. In SRM conditions, combustion of aluminum occurs at elevated temperatures (~2700–3000 K) and pressures (~40–100 atm). Modeling of the combustion of aluminum in this environment is essential to enhance the predictive ability for new propellant formulations, but any model of aluminum combustion must still rely on experimental data for validation. Accurate measurements of the fundamental behavior of aluminum combustion, such as the effects of oxidizer composition and pressure, are necessary to increase our knowledge of aluminum combustion as a basis for these models. In previous studies, most of the experimental measurements of aluminum combustion have taken place on relatively large particles and agglomerates. Although many advanced SRM propellant formulations use much finer aluminum than current formulations, little information is available on the combustion behavior of smaller particles, where a transition from diffusion-limited to kinetic-limited combustion is expected to occur.[1] If such a transition should occur, the dependence of burning time on oxidizer composition and on pressure can be dramatically different than what is observed for diffusion limited combustion.

Much research has been done to investigate the combustion timescales related to aluminum combustion and the dependence of these timescales on oxidizer composition. O_2, CO_2, and H_2O are the oxidizers most commonly thought to be significant in aluminum combustion. Oxygen is considered the strongest oxidizer, but the relative strength of CO_2 and H_2O, which are much more available than O_2 in a SRM, is less clear. Much of the research done on oxidizer effects has been done on the postflame gases of a gas burner or propellant mixture. This method does not provide independent control of oxidizer composition, and changing the concentration of one species also changes other key parameters, such as the concentration of other oxidizers and diluents and the temperature.

An overview of the work that has investigated oxidizer effects on aluminum combustion is presented as background information. Macek[2] looked at single 10–100-μm particles in the postflame gases of an atmospheric pressure burner. At the same partial pressure of oxygen, aluminum was found to burn faster in "dry" (no water vapor present) mixtures compared to "wet" mixtures. There is more CO_2 in the dry mixtures, and Macek attributes the difference in burn times as a result of H_2O replacing CO_2 in the mixture, indirectly suggesting that CO_2 is a stronger oxidizer that H_2O. Frolov et al.[3] examined the combustion rates of aluminum in different oxidizers by using a laboratory rocket motor and altering the propellant composition. They correlate experimental burn-time data from propellant tests to the inverse of the sum of H_2O and CO_2 concentrations (both oxidizers weighted the same) raised to 0.9 as shown in Eq. (1):

$$t_b \propto 1/a_k^{0.9} \tag{1}$$

where a_k is the sum of the water vapor and carbon-dioxide mole fractions. Therefore, their study concludes that CO_2 and H_2O oxidize aluminum at approximately the same rate. The 0.9 power indicates that the combustion time is also quite dependent on the concentration of oxidizer, with combustion time decreasing as oxidizer concentration increases.

Rossi et al.[4] compared the combustion of 165-μm particles burning at 1 atm in air with pure CO_2 using a pulsed micro-arc and found that the burn time was shorter in pure CO_2. Bucher et al.[5] show burn-time traces of approximately 130-μm laser-ignited particles falling in CO_2, H_2O, and O_2/Ar atmospheres at 1 atm. Although the primary point of the paper was to look at condensed phase species, they also report light intensity vs time. In their figures, O_2/Ar exhibits a sharp intensity peak with a tail. CO_2 has a strong rise and then decays. H_2O has an extended initial rise that is much longer than the other two oxidizers. Bucher et al. do not report burn time numbers, but the plots seem to indicate that aluminum burn times are fastest in O_2, followed by CO_2 and H_2O, respectively.

Beckstead et al.[6] have compiled much of the experimental burn-time information for aluminum combustion found in the literature and attempted to deduce the importance of oxidizer type, oxidizer concentration, particle diameter, pressure, and temperature in a correlation shown in Eq. (2):

$$t_b = d_o^{1.8} / 125\left(X_{O_2} + 0.6X_{H_2O} + 0.22X_{CO_2}\right) P^{0.1} T^{0.2} \tag{2}$$

where d_o is the original particle diameter, P is the pressure, and T is temperature in the surrounding environment. However, this study clearly shows that the scatter between experiments is large, and controlled experiments are needed to accurately determine these parameters. Also, very few data for small particles are available for

Received 9 August 2004; revision received 9 December 2004; accepted for publication 9 December 2004.

*Graduate Student, Mechanical and Industrial Engineering Department.
†Professor of Mechanical and Industrial Engineering. Fellow AIAA.
‡Associate Professor, Mechanical and Industrial Engineering. Member AIAA.

use in this correlation, and it is not known whether the correlation can be used for small particles.

Gremyachkin et al.[7] model the combustion of aluminum particles with an emphasis on the impact of heterogeneous reactions very near the particle surface, and their model predicts that oxygen is the strongest oxidizer, followed by water vapor and carbon dioxide, respectively. The difference in predicted burn times is primarily caused by the values of diffusion coefficient for each oxidizer.

In another model, Brooks and Beckstead[8] and Widener and Beckstead[9] predict the combustion times of aluminum under the influence of different oxidizers. The model extends Law's steady-state model[10] and includes multiple oxidizers and oxide accumulation on the surface. The burn time is also fit as inversely proportional to the weighted sum of oxidizers raised to the 0.39 power, as shown in Eq. (3) (Ref. 9):

$$t_b \propto 1 \Big/ \left(X_{O_2} + 0.58X_{H_2O} + 0.22X_{CO_2}\right)^{0.39} \tag{3}$$

The coefficients on the weighted sum are given as 1.0 for O_2, 0.58 for H_2O, and 0.22 for CO_2, meaning that oxygen is the strongest oxidizer, while H_2O is 0.58 times as effective as O_2, followed by CO_2 at 0.22 times as effective as O_2. The relative strength of the oxidizers is explained primarily as a result of heat of reaction of aluminum with each oxidizer and diffusion coefficient of each mixture. Olsen and Beckstead[11] attempt to verify this model experimentally using the postflame gases from a burner at 1 atm. Their data show a decrease in burn time when some CO_2 replaces H_2O, but the analysis does not take into account many other factors that change between runs, such as oxygen concentration and overall diffusion coefficient. Also, only two experimental conditions are used when testing the effect of oxidizer. Olsen and Beckstead[11] also attempt to fit the data of many other researchers to the effective oxidizer correlation given by Brooks and Beckstead,[8] but each of these measurements is taken using dramatically different techniques, temperatures, pressures, particle sizes, etc., and direct comparison between studies is difficult.

Models[12] and experimental results[13,14] have indicated that the flame structure of larger aluminum droplets also differs significantly with each oxidizer. Widener et al.[12] demonstrate that in numerical simulations the flame front is much closer to the surface in H_2O as compared to CO_2 and O_2. Also, the flame temperature is predicted to be lower in CO_2 as compared to the other oxidizers. Legrand et al.[13] show pictures of aluminum particle combustion in CO_2, where there is a flame zone that is close to the particle surface with a less luminous outer zone, as opposed to air where there is a bright outer flame region at least a few particle radii from the surface. Bucher et al.[14] show AlO and temperature profiles for aluminum particles burning in air and CO_2 atmospheres, and the flame is shown to be closer to the surface in CO_2 compared to air. These studies indicate that there is a significant difference in flame structure for aluminum for different oxidizers at these relatively large particle sizes. However, temperature measurements of fairly small, 10-μm particles indicate that the peak combustion temperature does not vary as significantly with oxidizer in this size range, with temperatures in the range of 3150–3300 K for all oxidizers.[15]

The dependence of burn time on pressure is also uncertain based on the available literature. Classically, diffusion of oxidizer to the particle is said to be proportional to the product of density, which is proportional to pressure, and diffusion coefficient, which is inversely proportional to pressure. Therefore, when diffusion controls burn rate, the burn rate is thought to be independent of pressure. Kudryavtsev et al.[16] argues that the presence of submicron condensed aluminum-oxide particles in the region surrounding the aluminum droplet can cause a decrease in diffusion that is pressure dependent. This would lead to burn time decreasing weakly with pressure. Studies[3,10,17] show that there is likely a weak dependence on pressure at large particle sizes when the pressure is relatively low ($<$20 atm) with no dependence at higher pressures.

In summary, even for larger particles that likely burn in a diffusion-limited fashion, there remains considerable uncertainty as to the relative oxidizer efficiencies of critical oxidizers, and there is almost no information on fine and ultrafine particles. A similar situation exists for the pressure dependence of the burning rate. There is clearly a critical need for highly controlled experiments of burning rate under varying pressure and oxidizer conditions, especially for fine particles.

Objectives

Using a heterogeneous shock tube, this study investigates the variation of burn time of small ($\sim$10 μm) aluminum particles with changes in oxidizer concentration and pressure. Unlike other methods of creating a hot, high-pressure environment relevant for aluminum combustion applications such as gaseous burners or propellant combustion products, the shock tube offers independent control of the parameters of the combustion environment. Because of the difficulty of measuring the burn time of small particles, there are relatively little data available for combustion times for particles smaller than 10 μm. Models have shown that as particles become smaller[18] surface processes (i.e., heterogeneous reaction rates, diffusion through oxide film) can affect burn performance, and this is in agreement with the basic theory of droplet combustion that predicts a transition to rate-limited burning at some small droplet diameter. Therefore, burn-rate laws that hold for large particles cannot necessarily be extended to the small particle regime. For that reason, this study will look at smaller particle sizes than previously examined, but still within the size range relevant for current and future SRM and explosives applications. The effects of pressure and oxidizer concentration will also be independently examined in this size regime.

Experiment

All of the experiments were performed in the University of Illinois at Urbana–Champaign heterogeneous shock-tube facility, which has been described in previous publications.[19,20] A schematic of its operation is shown in Fig. 1. In brief, an 8.38-m shock tube is used to generate a high temperature and elevated pressure environment behind the shock that is reflected off the shock-tube endwall. The temperatures for this study ranged from 2400–2700 K. The percentage of O_2, CO_2, and H_2O was varied between 20 and 60% with the remainder of gas being argon. For cases with water vapor, the shock tube was heated to 325 K to keep the driven gases in the vapor phase. The pressure behind the reflected shock was varied between 3–32 atm. The particles are ignited by the high temperatures in the region behind the reflected shock and burn in this oxidizing environment.

Particle injection was utilized in this study. A small sample of powder ($\sim$1 mg) is injected into the tube just after the tube is filled with gases of the requisite composition and just before the diaphragm is burst. The injector produces a dilute cloud of the particles, and this cloud is heated by the incident and reflected shocks. The particles burn in the tube under highly controlled temperature, pressure, and composition conditions. For these experiments, the particles were injected 1.4 m upstream of the endwall. The particles are entrained in the flow behind the incident shock and moved towards the endwall. The particles are then decelerated when the reflected shock passes by the stationary region behind the reflected shock. Combustion then occurs in this hot, quiescent region behind the reflected shock.

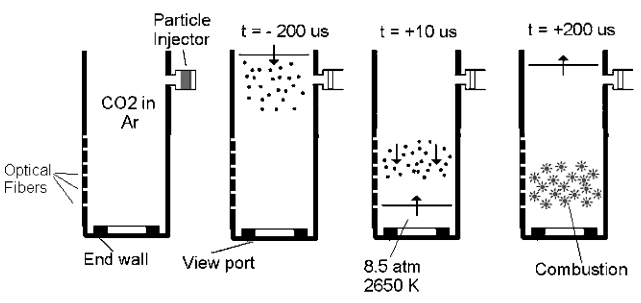

Fig. 1 Schematic of shock-tube operation.

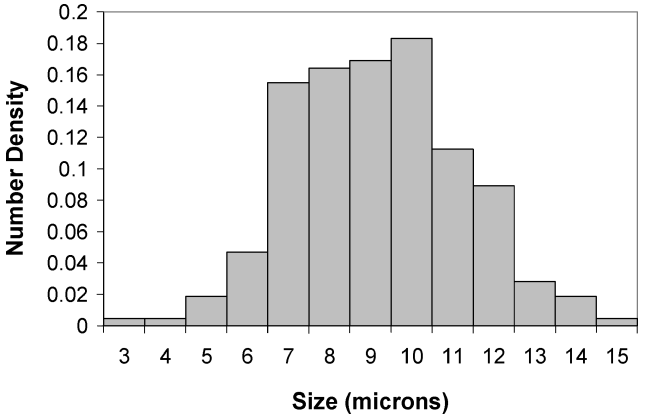

Fig. 2 Particle size distribution histogram of aluminum powder used in this study.

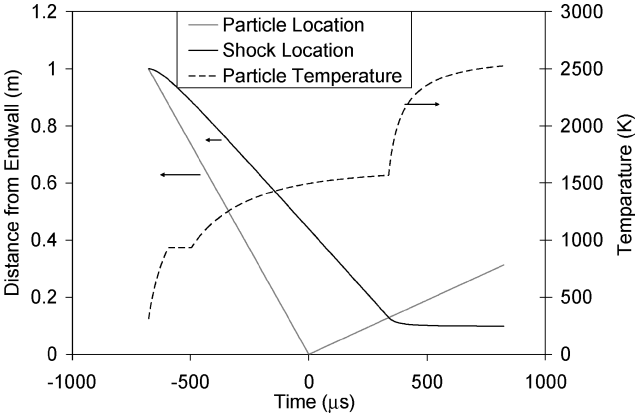

Fig. 3 Location of 10-μm particle, shock, and particle temperature vs time for a 10-μm aluminum particle in the shock tube.

The particles used in this study come from nominally 20-μm pure spherical aluminum powder purchased from Aldrich. The particles were size selected by sieving to be between 5–10 μm. A particle size distribution histogram of a sample of 240 particles is shown in Fig. 2. Analysis shows than the mean effective diameter for the particles is 9.2 μm with a standard deviation of 2.1 μm. Although the size distribution based on number seems fairly broad, more important to this study is the distribution of the light emission from each particle, which can be estimated as proportional to the particle mass, or diameter cubed. This mass distribution is narrower, with a fairly sharp peak around 10 μm. Therefore, the measurements of light emission performed in this study reflect the behavior of particles very near 10 μm in size.

The combustion event is observed through optical fibers mounted in the shock-tube wall shown in Fig. 1. The fibers can be mounted so that they have 6 mm spacing in the shock tube axial direction. The numerical aperture of the fibers is selected so that the fiber transmits only emission of light from the 6-mm axial region surrounding each fiber, matching the fiber spacing with the fiber resolution. Multiple experiments are completed at each condition. The emission signal vs time in the region surrounding the combustion is measured through the optical fibers using amplified photodiodes. AlO is a primary combustion intermediate of aluminum in all oxidizers. The presence of AlO indicates combustion is occurring, whereas lack of AlO signal indicates absence of combustion. AlO is also a very strong emitter at combustion temperatures, and the $\Delta v = 0$, $B - X$ transition of AlO centered at 486 nm emits brightly. Ten-nm bandpass interference filters centered at 486 nm are placed in front of the photodiodes, and so mainly emission from AlO is captured by the photodiode. The region of the cloud where the emission signal has the highest signal-to-noise ratio is then processed for a burn time. This corresponds to the region in the shock tube where the majority of injected cloud has come to rest, and therefore the behavior of this region represents the behavior of the average 9.2-μm aluminum particles.

Analysis

Although collection of emission intensity vs time is fairly straightforward and represents a valid measurement of burn time, some analysis must be done to account for a few factors in this experiment. First, the location and temperature history of the particles must be understood and analyzed. An analytical model of the particles' movement and heating was performed so that the position and temperature of the particles prior to ignition vs time could be predicted. The parameters of the shock and powder are input into the model, and the temperature and location history are produced, as shown in Fig. 3. The model assumes spherical aluminum particles suspended initially motionless in the shock tube. Particle trajectories are determined by determining the time-dependent drag force using a drag coefficient based on empirical data for C_D vs Re. The thermal history of the particles is obtained by a heat-transfer analysis that includes radiation, melting, and convection. The Nusselt number is

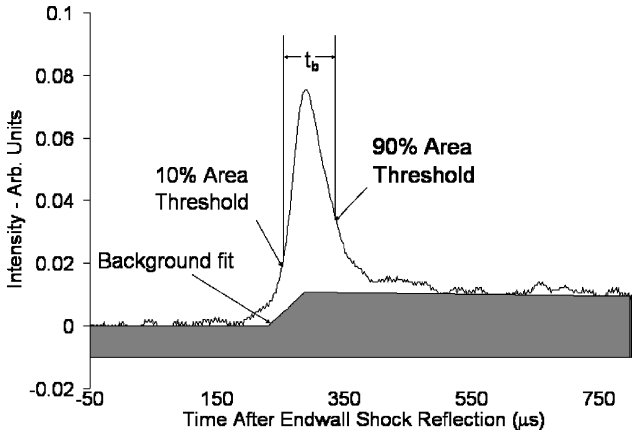

Fig. 4 Typical intensity signal at 486 nm for oxygen cases and background for area burn analysis.

calculated as a function of Re and Pr from an explicit expression for spherical particles.[21] For radiation, we assume an emissivity of one. Radiation effects are, in general, very small for these particles.

For each test, the model provided insight into the expected location and time of particle ignition. The burning particle location was compared to the location of brightest emission from the photodiode signals, and the results correlated very well. This indicates that the model captures the behavior of the majority of the particles in the flow and that the location of brightest signal corresponds to the location where the mean particle sizes burn. Photodiode signals were collected at five different axial locations for each run. The region around and slightly upstream of the region with peak emission intensity is used in the analysis of burn time. This choice removes the effects of agglomerated particles, which travel past this region, and particles entrained in the boundary layer of the tube walls, which do not reach this region.

Typical ways of quantifying burn time include constant intensity cutoff method, full-width at half-maximum or another percent height method, and percent total area method.[11] Because the burns often had multiple peaks, particularly at low oxidizer concentrations, the percent-area method provides the most unambiguous determination of burn time, and therefore the data presented here are processed by using the percent-total-area method. The burn time is therefore the time between 10 and 90% of the total integrated intensity signal, as illustrated in Fig. 4.

Because certain runs with lower signal levels exhibit appreciable thermal emission after combustion is complete, a background is fit to the intensity signal. Experiments[4] have shown that the thermal emission signal rises with or shortly after the AlO emission. Therefore, a background is fit to each intensity signal. Figure 4 shows this background fit to an intensity signal with appreciable thermal emission.

Particle movement during combustion, along with the finite field of view of the detector, leads to a systematic error in burn-time measurement. A correction is therefore applied to our measured data to account for this systematic error. This correction is necessary because the particles are initially heated at different times based on when they are passed by the reflected shock because of the spatial distribution of the particle cloud. Using the analytical model of particle movement and temperature, the estimated time difference between the first particle and last particle to ignite within the field of view is determined and subtracted from the measured burn time. The time difference can be approximated by Eq. (4):

$$t_{\text{cor}} = (D_{\text{FOV}} + D_{\text{move}})/V_{\text{shock}} \tag{4}$$

where t_{cor} is the correction to the burn time, D_{FOV} is the size of the field of view, D_{move} is the distance the particle moves after ignition as determined by the model, and V_{shock} is the reflected shock velocity.

A correction must also be made to account for the equilibrium composition in the reflected shock region. Although a certain composition is present in the low-temperature region before the shock, equilibrium chemistry leads to a different composition present in the region behind the reflected shock. For instance, if 50% CO_2 and 50% argon are present before the incident shock a certain amount of CO_2 will dissociate at the high temperatures behind the reflected shock (2650 K, 8.5 atm), and the resulting composition will be approximately 48%Ar, 42%CO_2, 7%CO, 3%O_2, and trace amounts of other species. Therefore, the oxidizing ability of these other gases must be considered. The equilibrium composition can be easily calculated behind the reflected shock using one of many standard computer programs. Equilibrium is reached well within 100 μs, before combustion begins.

As a first-order correction, the total burn rate (1/burn time) is assumed to be the result of the sum of the burn rates as a result of each oxidizer present, that is, the observed burn rate is composed of the burn rate caused by the primary oxidizer (CO_2 in the preceding example) and the burn rate caused by the other oxidizing species (CO, O_2, and other trace species in the example). This relation is similar to that assumed in Eq. (2) (Ref. 9). Although there are possibly effects that cause acceleration of combustion when using multiple oxidizers and this relation should not be extended to other oxidizer mixtures, the simple approach of adding burn rates can be used as a first-order correction for the small concentrations of the secondary oxidizers observed in this study.

In oxygen cases, the only the oxidizers present in significant amounts are O_2 and O. In the absence of other data, we assume that O atoms react on approximately the same timescale as O_2. Because the O mole fraction is typically two orders of magnitude smaller than that of O_2 at elevated temperatures, this assumption likely has little effect on the overall results of the study. Therefore, the oxygen cases can be processed, and a correlation between burn time and oxygen concentration can be established. To analyze the burn time in CO_2 and H_2O, the other minor oxidizing species present in the mixture (O, O_2, and OH) are assumed to react on similar timescales to oxygen gas. The mole fractions of these species are summed, and the reaction rate caused by these species is estimated by extrapolation of the oxygen data. This reaction rate is subtracted from the observed reaction rate, giving the corrected reaction rate vs mole fraction for the primary oxidizer. To estimate the oxidizing ability of CO, tests with only CO as the oxidizer were performed. Forty-percent CO environments do produce reaction, but the burn times are much longer than the test time of the shock tube. The reaction rate caused by CO is thus assumed to be insignificant compared to the other oxidizers when they are present in appreciable quantities. This correction is applied for each test based on the equilibrium conditions in the shock tube for that particular run.

Both the particle movement and oxidizer correction become 0–20% corrections to the burn time, but they also act in opposite directions to give a canceling effect, as the particle movement corrections increase reaction rates while the oxidizer correction lessens reaction rates. Thus, the overall correction to the measured burn time remains in the 0–20% range.

The uncertainty in the measurement is a combination of the measured statistical variation and the uncertainty in the measurement and corrections. Multiple runs are used for each data point, with multiple detectors utilized for each run, giving over 10 analyzed photodiode signals for each data point. The one-sigma standard deviation in these measurements is added in quadrature to the uncertainties caused by the movement and composition corrections. In relative terms, the correction for particle movement typically accounts for about 0–25% of the total uncertainty, the correction for oxidizer composition typically accounts for 0–50%, and the statistical variation typically accounts for 0–50% of the uncertainty.

Results

Burn-time data were collected for O_2, CO_2, and H_2O in the range of 20–60% of each oxidizer in an argon diluent at temperatures close to 2650 K and 8–10 atm. At lower oxidizer concentrations, the combustion event lasted longer than the test time of the shock tube, approximately 1.7 ms. Figure 5 shows the results for corrected burn time vs effective fraction of primary oxidizer. The error bars represent the uncertainty as discussed in the preceding section. The mole fraction of primary oxidizer is the equilibrium mole fraction of the primary oxidizer in the reflected shock region. The general trend of the data series agrees with theory and previous work, with the burn time decreasing as the mole fraction oxidizer increases. It can also be seen that aluminum has the fastest burn time in oxygen followed by carbon dioxide and water vapor, respectively.

The data can be correlated by a relation similar to those used in the literature[3,8,9] of the following form:

$$t_b = 1 \Big/ C_{\text{ox}} X_{\text{ox}}^n \tag{5}$$

where t_b is the burn time, X_{ox} is the mole fraction of oxidizer, and C_{ox} and n are empirical constants. Using this correlation, the data presented in Fig. 5 can be fit to the empirical constants shown in Table 1.

The different oxidizers would not necessarily be expected to fit to the same exponent n because of fundamental differences in the processes involved with the combustion in each respective oxidizer. However, this practice has been done previously, and so for the sake of comparison the data are fit to a similar correlation as Eq. (5) with the exponent fixed at unity, similar to Ref. 6. Also the constant C are normalized to the oxygen constant to gauge the relative strength of each oxidizer. The values for C then become $C_{O2} = 1$, $C_{CO2} = 0.56$, and $C_{H2O} = 0.26$.

Table 1 Empirical constants for the correlation of burn-time oxidizer mole fraction

Oxidizer	O_2	H_2O	CO_2
C [1/μs]	0.0157	0.0094	0.0102
n	0.94	2.1	1.08

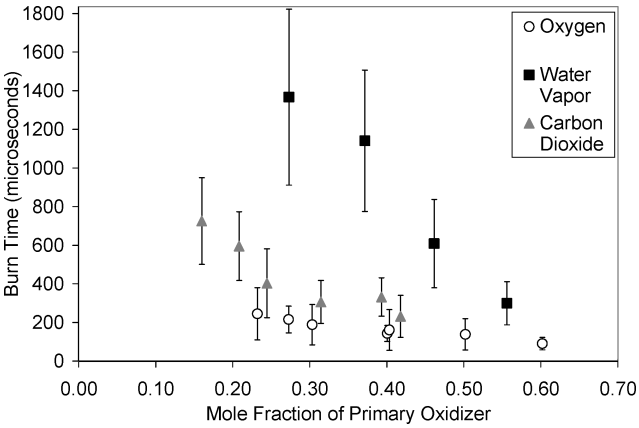

Fig. 5 Burn time corrected for particle movement and alternate oxidizers vs the mole fraction of the primary oxidizer at 8.5 atm.

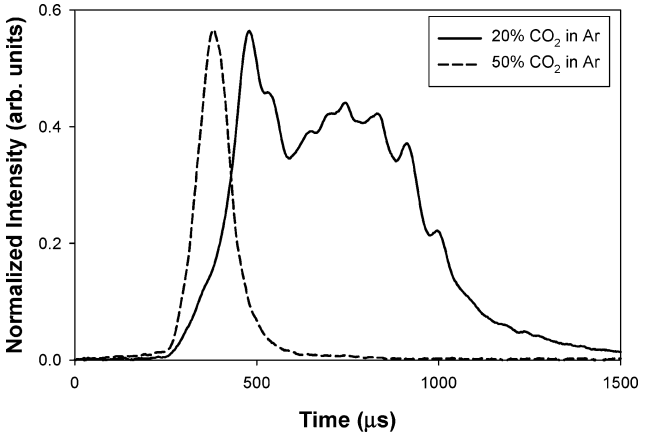

Fig. 6 Representative photodiode signals at 486 nm for aluminum powder in 50 and 20% CO_2 in argon.

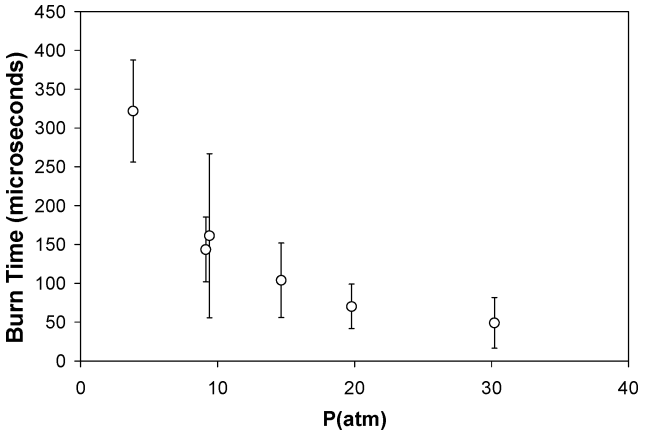

Fig. 7 Burn time vs pressure for 40% O_2.

There is a change in the structure of the intensity vs time plots as oxidizer fraction decreases. At high oxidizer fractions, the intensity signal tends to be fairly straightforward, with a simple rise and fall structure. As oxidizer fraction decreases, the intensity vs time plots exhibit a fairly sharp initial rise followed by multiple peaks before decaying. This phenomenon is displayed in Fig. 6, which shows representative intensity vs time signals for aluminum burning in 20% CO_2 and 50% CO_2 with the balance argon. The difference in shape between the high- and low-oxidizer mole fraction could be indicative of the transition from kinetic to diffusion-limited combustion as oxidizer becomes less available and transport becomes more important.

Burn-time data were also measured with variable pressure while gas composition and temperature are held constant for each of the three oxidizers. For our shock-tube facility, pressures could be varied in the range 3–32 atm for oxygen and carbon-dioxide atmospheres and in the range 3–15 atm for water vapor because of limitations of the vapor pressure for water in the preshock environment. For 40% O_2/60% Ar atmospheres, the burn time vs pressure data are displayed in Fig. 7. As shown, the burn time is strongly related to pressure in this regime, with burn time decreasing dramatically while pressure increases. This relationship can be empirically fit as $t_b \sim 1/P^{0.9}$ for 3 atm $< P <$ 30 atm.

Figure 8 shows burn time vs pressure data for aluminum burning in 32% CO_2. As can be seen, the data for carbon dioxide do not follow the same trend observed in oxygen, but rather the burn time has a weak increase with increasing pressure. The pressure appears to be approaching a plateau region as we move to higher atmospheres. The dependence is less strong than oxygen, with the appropriate fit $t_b \sim P^{0.3}$. Figure 9 shows the burn time vs pressure data for aluminum burning in 50% H_2O, which also exhibits the weak increase in burn time with increasing pressure. The corresponding power law fit for these data is $t_b \sim P^{0.2}$. A clear contrast can be noted between the behavior of both carbon dioxide and water vapor as opposed to oxygen.

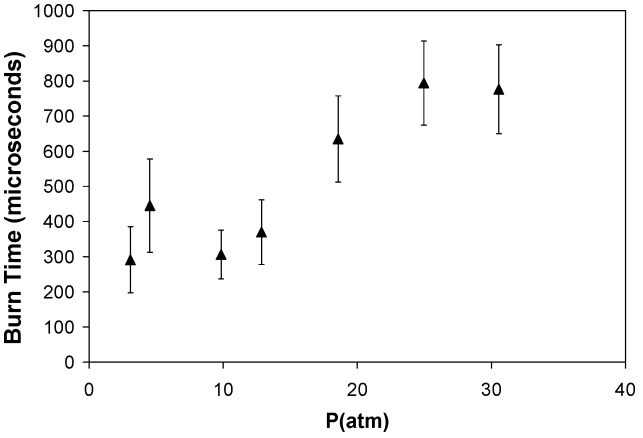

Fig. 8 Burn time vs pressure data for aluminum in 32% CO_2.

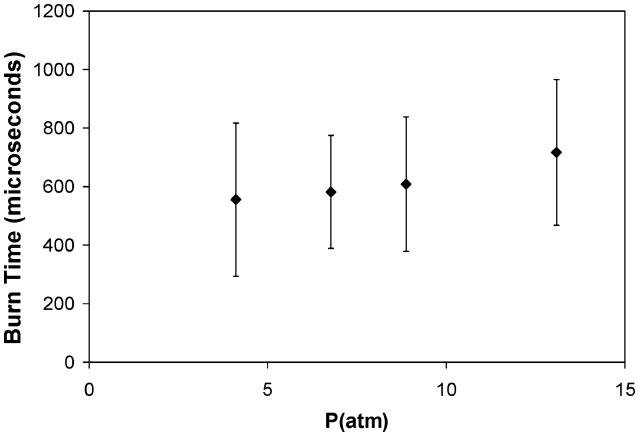

Fig. 9 Burn time vs pressure data for aluminum in 50% H_2O.

Discussion

The burn times measured here are within the range of expected values. However, because the previous research exhibits significant variation among the various proposed correlations,[3,6,9,10] it is difficult to compare any particular correlation. Most of the correlations and extrapolations use a d^n law, with n between 1.5 and 2, to predict a burn time for 10-μm particles to be somewhere in the range of 200–2000 μs, depending on the study. The results observed here are within this wide range of possible values, but it is also clearly impossible to determine if the d^n laws can be extrapolated to particles in this size regime because of the scatter observed in the available correlations.

For 10-μm particles, the burn-time data indicate that burn time decreases dramatically with increasing oxidizer concentration. This is to be expected, as more oxidizer is available for reaction with aluminum, thus allowing faster reaction. In general, the shape of the curves matches up reasonably well with experimental findings and models for larger particles. Comparison for curve shape can be found various references,[3,6,7] and virtually all references predict the shape resembling an inverse relationship between burn time and concentration.

We do not find that all oxidizers react at similar rates, even for CO_2 and H_2O as proposed by Frolov et al.[3] Studies that compare the relative oxidizers for larger size particles[5,8,10,11] indicate that oxygen is the strongest common oxidizer. However, as stated in the Introduction, there is still uncertainty in the literature about the relative strengths of carbon dioxide and water vapor. This study clearly shows that for 10-μm particles, where the oxidizer concentrations are varied independently, burn times are faster in CO_2 compared to H_2O. If water vapor is indeed the stronger oxidizer for large particles that burn in a diffusion-limited fashion, caused at least in part

by its higher diffusion coefficient, there is no reason to expect it to continue to be the faster oxidizer for small particle diameters in which surface kinetics can play the controlling role.

The difference in the pressure dependence of aluminum burn times is somewhat surprising. As stated in the Introduction, the classical view is that burn time is independent of pressure to first order. The large dependence of burn time in oxygen on pressure contradicts this idea. This observed effect could also be indicative of combustion limited by a surface process, in which the rate of diffusion of oxidizer to the surface would no longer control the combustion rate. Combustion theory dictates that as particles get smaller kinetic rates will become more important in the combustion process. For a simple first-order reaction at the surface, one would expect in a kinetic-limited regime that the burning rate would increase inversely with pressure. Such dependence is approximately what we observe in oxygen-containing environments for this particle size range.

The pressure dependence of both carbon dioxide and water vapor does not exhibit this dramatic dependence, but rather shows a slight increase with pressure. This contradicts the theory of Kudryavtsev et al.,[16] which predicts a slight decrease with pressure. Increasing burn times with pressure have occasionally been observed for large particles in certain environments, for example, the experiments of Marion et al.[17] between 1 and 1.5 MPa, although even the general trend of their data is a decrease with burn time. Though a definitive explanation cannot be advanced at this time, equilibrium analysis suggests the possibility of a critical role of a secondary species. In the high-temperature region near the particle surface, CO_2 and H_2O will further dissociate to form more reactive oxides (e.g., O, OH, O_2), but this dissociation is inhibited at elevated pressure. If these minor species play important roles in the oxidation chain involving H_2O and/or CO_2, then it might be expected that there is an inverse dependence on pressure.

Of particular interest is the difference in pressure dependence between oxygen and the other oxidizers. The weak dependence of burn time for carbon dioxide and water vapor is more typical to the diffusion-limited combustion typically observed for larger particles. As stated earlier, the strong dependence on pressure for oxygen might be a sign that kinetics could be playing a role in the combustion process. This observed phenomenon might be indicative of the fact that the diffusion to kinetic transition will occur at different size regimes for different oxidizers. Although oxygen produces the fastest burn times and presumably has the fastest kinetics, this does not necessarily preclude the kinetics being more prevalent for oxygen and diffusion more prevalent for CO_2 and H_2O. For each O_2 molecule that diffuses to the particle surface, two oxygen atoms will be available to react with aluminum, whereas only one oxygen atom will be available to react for both CO_2 (assuming the formation of CO) and H_2O. Therefore, diffusion will have to occur twice as fast in CO_2 and H_2O to produce the same amount of oxygen for reaction with aluminum. Because of the increased oxygen atoms transported to surface with oxygen gas, kinetics could become important in O_2 environments, whereas diffusion remains more important in CO_2 and H_2O environments.

The possibility exists that the particles do not burn to completion during the combustion event, and, if so, this would alter the interpretation of oxidizer strength. Because of the great amount of debris in the shock tube created by the diaphragm and the small injected charge, recovering uncontaminated samples for ex situ analysis is likely impossible. However, in all cases pyrometry measurements show that the particles rise to an elevated temperature above the 2650 K ambient during combustion, then decay to the ambient temperature after the burn but still well within the test time. The fact that the product particles remain inert in a high-temperature oxidizing environment that is well above the ignition threshold and alumina melting point suggests that little aluminum remains in these particles.

Conclusions

A method was devised to record burn times accurately for 10-μm spherical aluminum particles. The shock tube allows for the independent variation of both oxidizer composition and pressure. Burn time decreases strongly with increasing oxidizer mole fraction. The oxidizing species plays a significant role in determining burn time, with oxygen producing the shortest burn time followed by carbon dioxide and water vapor, respectively. The pressure dependence of burn time was also found to be very dependent on oxidizer. This work looks at combustion of smaller particles than have previously been observed extensively, and results suggest that surface processes could become more significant for particles in the 10-μm and smaller size regime.

Acknowledgment

This work has been supported by the Office of Naval Research under Contract N00014-01-1-0899. The project monitor is Judah Goldwasser.

References

[1]Glassman, I., *Combustion,* 3rd ed., Academic Press, San Diego, CA, 1996, Chap. 9.

[2]Macek, A., "Fundamentals of Combustion of Single Aluminum and Beryllium Particles," *Proceedings of the 11th Symposium (International) on Combustion*, Vol. 7, Combustion Inst., Pittsburgh, PA, 1967, pp. 203–217.

[3]Frolov, Yu. P., Pokhil, P. F., and Logachev, V. S., "Ignition and Combustion of Powdered Aluminum in High-Temperature Gaseous Media and in a Composition of Heterogeneous Condensed Systems," *Fizika Goreniya i Vzryva,* Vol. 8, No. 2, 1972, pp. 213–236.

[4]Rossi, S., Dreizin, E. L., and Law, C. K., "Combustion of Aluminum Particles in Carbon Dioxide," *Combustion Science and Technology,* Vol. 164, Nos. 1–6, 2001, pp. 209–237.

[5]Bucher, P., Yetter, R. A., Dryer, F. L., and Vicenzi, E. P., "Condensed-Phase Species Distributions About Al Particles Reacting in Various Oxidizers," *Combustion and Flame,* Vol. 117, No. 1–2, 1999, pp. 351–361.

[6]Beckstead, M. W., Newbold, B. R., and Waroquet, C., "A Summary of Aluminum Combustion," *50th JANNAF Propulsion Meeting*, Chemical Propulsion Information Agency Publication 705, Vol. 1, 2001, pp. 201–220.

[7]Gremyachkin, V. M., Istratov, A. G., and Leipunskii, O. I., "Model for the Combustion of Metal Droplets," *Fizika Goreniya i Vzryva,* Vol. 11, No. 3, 1975, pp. 313–318.

[8]Brooks, K. P., and Beckstead, M. W., "Dynamics of Aluminum Combustion," *Journal of Propulsion and Power,* Vol. 11, No. 4, 1995, pp. 769–780.

[9]Widener, J. F., and Beckstead, M. W., "Aluminum Combustion Modeling in Solid Propellant Combustion Products," AIAA Paper 98-3824, July 1998.

[10]Law, C. K., "A Simplified Theoretical Model for the Vapor-Phase Combustion of Metal Particles," *Combustion Science and Technology,* Vol. 7, No. 5, 1973, pp. 197–212.

[11]Olsen, S. E., and Beckstead, M. W., "Burn Time Measurements of Single Aluminum Particles in Steam and CO2 Mixtures," *Journal of Propulsion and Power*, Vol. 12, No. 4, 1996, pp. 662–671.

[12]Widener, J. F., Liang, Y., and Beckstead, M. W., "Aluminum Combustion Modeling in Solid Propellant Environments," AIAA Paper 99-2629, June 1999.

[13]Legrand, B., Marion, M., Chauveau, C., Gokalp, I., and Shafirovich, E., "Ignition and Combustion of Levitated Magnesium and Aluminum Particles and Carbon Dioxide," *Combustion Science and Technology,* Vol. 165, No. 1, 2001, pp. 151–174.

[14]Bucher, P., Yetter, R. A., Dryer, L., Parr, T. P., and Hanson-Parr, D. M., "PLIF Species and Ratiometric Temperature Measurements of Aluminum Particle Combustion in O2, CO2, and N2O Oxidizers, and Comparison with Model Calculations," *Proceedings of the 27th Symposium (International) on Combustion*, Vol. 27, Combustion Inst., Pittsburgh, PA, 1998, pp. 2421–2429.

[15]Glumac, N., Krier, H., Bazyn, T., and Eyer, R., "Temperature Measurements of Aluminum Particles Burning in Carbon Dioxide," *Combustion Science and Technology* (in press).

[16]Kudryavtsev, V. M., Sukhov, A. V., Voronetskii, A. V., and Shpara, A. P., "High-Pressure Combustion of Metals," *Fizika Goreniya I Vzryva,* Vol. 15, No. 6, 1979, pp. 50–57.

[17]Marion, M., Chauveau, C., and Gokalp, I., "Studies on the Ignition and Burning of Levitated Aluminum Particles," *Combustion Science and Technology*, Vol. 115, No. 4–6, 1996, pp. 369–390.

[18]King, M. K., "Modeling of Single Particle Aluminum Combustion in CO2-N2 Atmospheres," *Proceedings of the 17th Symposium (International) on Combustion*, Vol. 17, Combustion Inst., Pittsburgh, PA, 1977, pp. 1317–1328.

[19]Servaites, J., Krier, H., Melcher, J. C., and Burton, R. L., "Ignition and Combustion of Aluminum Particles in Shocked $H_2O/O_2/Ar$ and $CO_2/O_2/Ar$ Mixtures," *Combustion and Flame,* Vol. 125, No. 1–2, 2001, pp. 1040–1054.

[20]Bazyn, T., Eyer, R., Krier, H., and Glumac, N., "Combustion Characteristics of Aluminum Hydride at Elevated Pressure and Temperature," *Journal of Propulsion and Power,* Vol. 20, No. 3, 2004, pp. 427–431.

[21]Incropera, F. P., and Dewitt, D. P., *Fundamental of Heat and Mass Transfer*, 4th edition, Wiley, New York, 1996, p. 374.